Simultaneously phase-matched second- and third-harmonic generation from 1.55 μm radiation in annealed proton-exchanged periodically poled lithium niobate waveguides

M. Marangoni, M. Lobino, and R. Ramponi

Dipartimento di Fisica-Politecnico and IFN-CNR, Piazza L. da Vinci 32, 20133 Milan, Italy

Received March 23, 2006; revised June 22, 2006; accepted June 27, 2006;
posted July 5, 2006 (Doc. ID 69311); published August 25, 2006

Third-harmonic generation (THG) in the cw regime from *C*-band radiation was achieved in annealed proton-exchanged periodically poled lithium niobate (PPLN) waveguides. By suitable design of fabrication parameters and operating conditions, quasi-phase-matching (QPM) is obtained simultaneously for the second-harmonic generation process ($\omega \rightarrow 2\omega$, first-order QPM) and for the sum-frequency-generation process ($\omega + 2\omega \rightarrow 3\omega$, third-order QPM), which provides the third harmonic of the pump field. The high overlap between the field profiles of the interacting modes—TM_{00} at ω and TM_{10} at 2ω and 3ω—results in what is believed to be the highest ever reported normalized conversion efficiency for THG from telecommunication wavelengths, equal to 0.72% $W^{-2}\,cm^{-4}$. © 2006 Optical Society of America

OCIS codes: 190.4160, 130.4310, 300.6460.

In several scientific areas, ranging from optical communication systems[1] to fundamental physical constant measurement,[2] frequency-stabilized sources are required for the realization of optical frequency standards.[3] The frequency stabilization is generally obtained by locking the laser frequency to an atomic or a molecular absorption line. Techniques such as saturation spectroscopy are employed to obtain stabilization to a sub-Doppler level, where absorption lines with natural spectral widths at the megahertz level are accessible.

For a given laser source that is to be stabilized, however, strong and sharp absorption lines might be missing at the laser frequency but still be available at double or triple that frequency. Therefore there is a need for new and efficient optical mixing schemes that are able to connect frequencies in 1:2 and 1:3 ratios compatible with low-power cw frequency stabilized lasers. The most efficient schemes for connecting frequencies are obtained by combining quasi-phase-matched nonlinear interactions, in either periodic[4,5] or quasi-periodic structures,[6,7] with guided propagation.[8] Semiconductor lasers in the 1.55 μm range have been recently stabilized[9,10] at a kilohertz level by locking the second harmonic, generated in periodically poled lithium niobate (PPLN) waveguides, to absorption lines of Rb and I_2 in the near-IR spectral range. A higher degree of stabilization, below the kilohertz level, could be obtained with the third harmonic, since in the green spectral range the I_2 molecule presents its strongest and sharpest lines. Until now, however, no efficient third-harmonic generation (THG) has been obtained in guiding structures,[11] owing to the difficulty of phase matching a three-wave mixing process, consisting of cascaded second-harmonic generation (SHG, $\omega \rightarrow 2\omega$) and sum-frequency generation (SFG, $\omega + 2\omega \rightarrow 3\omega$).

In this Letter we report the design, realization, and characterization of an annealed proton-exchanged (APE) PPLN waveguide where THG of *C*-band radiation is achieved at a fixed temperature as a result of quasi-phase-matched cascaded SHG and SFG. The frequency conversion is obtained with a normalized internal efficiency of 0.72% $W^{-2}\,cm^{-4}$, which is to our knowledge the highest value reported to date in the literature.

Frequency tripling is not trivial in a channel waveguide configuration, since two phase-matching conditions have to be simultaneously satisfied, the first one for the SHG process, the second one for the SFG process:

$$\Delta\beta^{\mathrm{SHG}} = \frac{4\pi}{\lambda}(n^{2\omega} - n^{\omega}) - r\frac{2\pi}{\Lambda} = 0,$$

$$\Delta\beta^{\mathrm{SFG}} = \frac{2\pi}{\lambda}(3n^{3\omega} - 2n^{2\omega} - n^{\omega}) - s\frac{2\pi}{\lambda} = 0, \qquad (1)$$

where n are the effective indices of the interacting modes, λ is the pump wavelength, Λ is the poling period of the crystal, and r, s are the quasi-phase-matching (QPM) orders for the two processes. The effective indices at the three frequencies depend both

Table 1. Design Parameters for a Waveguide Giving Phase-Matched THG[a]

Λ (μm)	A (μm)	λ_{pm}^{THG} (nm)	d_{pm}^{THG} (μm)	Δn_{pm}^{THG}
18.6	0.052	1550.3	1.95	0.02677
	0.056	1551.5	2.10	0.02667
	0.060	1552.6	2.24	0.02678
18.9	0.052	1560.6	1.77	0.02938
	0.056	**1561.9**	**1.92**	**0.02917**
	0.060	1563.1	2.06	0.02912

[a] Λ, poling period; $A = d_{pm}^{THG}\Delta n_{pm}^{THG}$; d_{pm}^{THG}, optical depth; Δn_{pm}^{THG}, index change at 633 nm; λ_{pm}^{THG}, phase-matching wavelength.

0146-9592/06/182707-3/$15.00

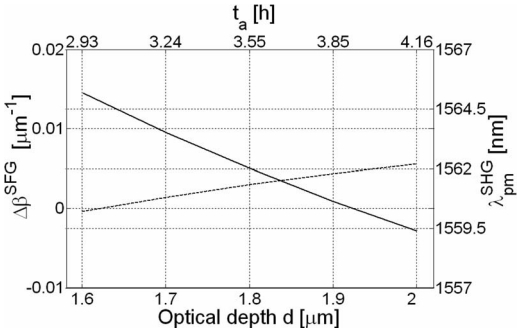

Fig. 1. Phase mismatch of the SFG process (solid curve, left-hand axis) and phase-matching wavelength of the SHG process (dashed curve, right-hand axis) calculated versus optical depth (lower scale) and corresponding total annealing time (upper scale).

on the operating conditions, i.e., pump wavelength and crystal temperature, and on the waveguide optical parameters defining the refractive index profile. Since single-mode APE waveguides exhibit optical depths 2–5 times smaller than typical channel widths, the dependence of the effective indices on the channel width was neglected in the design of a waveguide satisfying Eqs. (1). Only the parameters defining the transverse index profile were thus considered, i.e, the optical depth d and the index change at the surface Δn.

The following constraints were taken into account in the design: (i) first-order QPM ($r=1$) for the SHG process, and first available order, i.e., the third one ($s=3$), for the SFG process; (ii) phase-matching wavelength for the THG process (λ_{pm}^{THG}) in the C band; (iii) single-mode propagation at the pump wavelength; (iv) phase-matching temperature around 120°C, so as to avoid photorefractive effects; and (v) waveguide optical parameters compatible with the presence of an α crystallographic phase in the APE region, which is essential for reaching the best linear and nonlinear optical properties.[12] It is worth recalling that, once the α crystallographic phase is reached during the annealing, the index profile can be described by an exponential curve with a maximum value Δn at the surface and a $1/e$ optical depth d, where the product $A=d\Delta n$ is almost constant and is related mainly to the proton-exchange duration.[12]

The constraints pointed out above limit the choice of the order of the interacting modes to few configurations, the most efficient one involving TM_0 at ω, TM_1 at 2ω, and TM_1 at 3ω (TM_{00}, TM_{10}, and TM_{10}, respectively, in the experimental channel configuration). By keeping this modal configuration and a temperature of 120°C fixed, we calculated, as a function of the poling period Λ and of the A parameter, the values $d$and Δn satisfying Eqs. (1) (hereafter called d_{pm}^{THG} and Δn_{pm}^{THG}), and the corresponding phase-matching wavelength λ_{pm}^{THG}. Table 1 reports the results obtained for three different values of A giving single-mode propagation at ω and for two poling periods providing phase matching in the C band. The poling period determines, independently from the A value, both λ_{pm}^{THG} and Δn_{pm}^{THG}, and thus the chromatic dispersion coefficient. In all cases Δn_{pm}^{THG} corresponds to the α crystallographic phase. From Table 1 it emerges that different combinations of parameters exist, fulfilling the constraints for THG. We chose those shown in bold ($A=0.56$ μm, $\Lambda=18.9$ μm, $\Delta n=0.0292$, $d=1.92$ μm), which correspond to a proton-exchange time of 1 h and an annealing time of 3 h 54 min under our experimental conditions, i.e., 247°C in 1% diluted benzoic acid melt and 350°C in air, respectively. For such a proton-exchange duration Fig. 1 shows the evolution of the phase mismatch $\Delta\beta^{SFG}$ as a function of the optical depth d (lower horizontal scale) and of the corresponding annealing time (upper horizontal scale): $\Delta\beta^{SFG}$ was calculated by assuming a pump wavelength yielding phase matching for the SHG process, also reported in the figure as λ_{pm}^{SHG}. With increased annealing time, $\Delta\beta^{SFG}$ reduces monotonically and vanishes for $d=d_{pm}^{THG}$, while λ_{pm}^{SHG} increases in a quite restricted interval of few nanometers.

The PPLN sample used in the experiments is 1.8 cm long, has a 18.9 μm poling period, and includes several channels having widths w from 6 to 10 μm. Because of the critical dependence of the phase mismatch $\Delta\beta^{SFG}$ on the annealing time (see Fig. 1), after proton exchange the sample was annealed by subsequent steps, monitoring the resulting $\Delta\beta^{SFG}$ after each step. To this aim the light from two distinct tunable cw laser sources was simultaneously coupled with a 60% efficiency into the waveguides, one laser emitting at λ_{pm}^{SHG} and amplified by an erbium-doped fiber amplifier to provide a strong 2ω field, the other one being tuned to the wavelength $\bar{\lambda}_{pm}^{SFG}$ providing phase matching to the nondegenerate SFG process $2\omega+\bar{\omega}$, $\bar{\omega}$ being its frequency. The difference $\Delta\lambda=\lambda_{pm}^{SHG}-\bar{\lambda}_{pm}^{SFG}$ vanishes once a degenerate quasi-phase-matched SFG process is established, and it is to a first order directly proportional to $\Delta\beta^{SFG}$. Figure 2 shows the experimental values of $\Delta\lambda$ and λ_{pm}^{SHG} for $T=120$°C, $w=8$ μm, and $\Lambda=18.9$ μm as a function of annealing time (t_a) and optical depth, the latter being determined after each annealing step by prism characterization of the planar waveguide formed on the opposite side of the sample. The re-

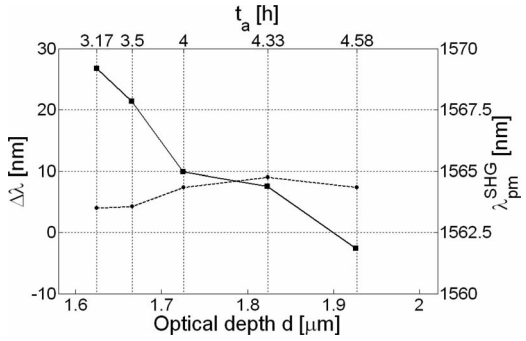

Fig. 2. Phase-matching-wavelength detuning from degenerate SFG (squares, left-hand axis) and phase-matching wavelength of the SHG process (circles, right-hand axis) measured versus optical depth (lower scale) and corresponding total annealing time (upper scale).

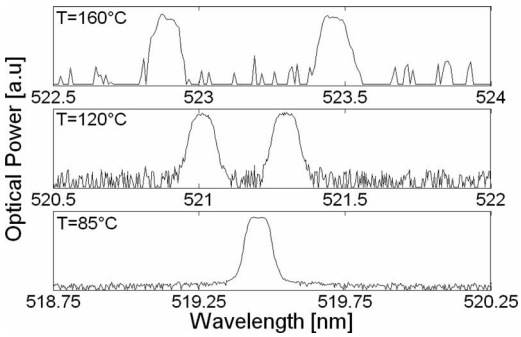

Fig. 3. Output spectra at three different temperatures: the leftward peaks are due to a phase-matched nondegenerate SFG process, the rightward to a phase-mismatched degenerate SFG process.

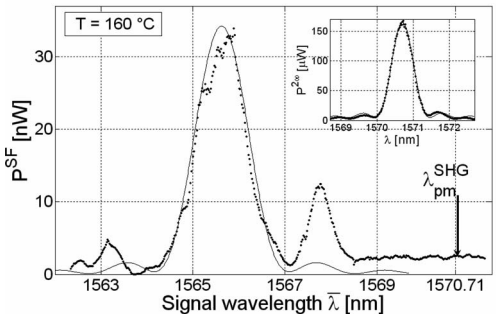

Fig. 4. Experimental (dotted curve) and calculated (solid curve) output power of the sum-frequency field (P^{SF} in the figure) as a function of the signal wavelength $\bar{\lambda}$ for an input pump power of 16 mW, a signal power of 16 mW, and a pump wavelength of 1570.7 nm. Inset, phase-matching curve of the SHG process in the same channel and for the same pump power. The second- and third-harmonic peak powers are 168 μW and 34 nW, respectively.

sults are in good agreement with the design predictions, the difference in the total annealing time being due to the thermal transients caused by the stepped process. When the annealing time is increased, the $\Delta\lambda$ value decreases and changes its sign when passing from 4 h 20 min to 4 h 35 min, thus indicating the need for tuning the waveguide temperature to achieve a phase-matched THG process. The output spectra at three different temperatures are reported in Fig. 3: at 160°C and 120°C two peaks are observed, the left-hand one due to the phase-matched nondegenerate SFG process, the right-hand one corresponding to the third harmonic generated under phase-mismatched conditions through the degenerate SFG process. The two peaks coincide at 85°C, thus attesting simultaneous SHG and degenerate SFG, and thus THG.

The conversion efficiency and the interaction length of the SFG process were studied by measuring the optical power of the sum-frequency field as a function of the wavelength $\bar{\lambda}$ at a temperature of 160°C (which implies a pump field at 1570.7 nm). This temperature was chosen to characterize the two processes independently. The experimental data, reported in Fig. 4 as a dotted curve, are fitted by a theoretical (solid) curve consistent with an effective interaction area of 137 μm^2, corresponding to a 29% $W^{-1}\,cm^{-2}$ normalized SFG efficiency and an interaction length of 6 mm, i.e., one third of the sample length. In contrast, the phase-matching curve for the SHG process, shown in the inset of Fig. 4, indicates a full 18 mm interaction length and an effective area of 98 μm^2 (20% $W^{-1}\,cm^{-2}$ normalized SHG efficiency). The waveguide homogeneity is thus not sufficiently high to maximize the interaction length of the SFG process, whose phase-matching condition is more critical. It is worth noting that for a THG process whose interaction length is shorter than the SHG process the third-harmonic power strongly depends on where the interaction region for THG is situated, because the second-harmonic beam feeding the SFG process increases its power while propagating. In our case this region was situated at the middle of the sample, since the optical power of the sum frequency was found to be independent of the propagation direction.

In conclusion, a quasi-phase-matched guided THG process was demonstrated in an APE PPLN dielectric structure. The normalized internal efficiency of the process, i.e., 0.72% $W^{-2}\,cm^{-4}$, is sufficiently high to predict, in an ideal waveguide exhibiting a 30 mm interaction length, the generation of 1 mW green light from 120 mW telecommunications radiation. This would allow subkilohertz frequency stabilization of laser sources in the *C* band by exploiting sub-Doppler green lines of the I_2 molecule.

This study was financially supported by MIUR through the FIRB project "Miniaturized Systems for Electronics and Photonics."

References

1. "Optical interfaces for multi-channel systems with optical amplifiers," ITU-T Recommendation G.962 (1998).
2. P. Cancio Pastor, G. Giusfredi, P. De Natale, G. Hagel, C. de Mauro, and M. Inguscio, Phys. Rev. Lett. **92**, 023001 (2004).
3. J. L. Hall, IEEE J. Sel. Top. Quantum Electron. **6**, 1136 (2000).
4. O. Pfister, J. S. Wells, L. Hollberg, L. Zink, D. A. Van Baak, M. D. Levenson, and W. R. Bosenberg, Opt. Lett. **22**, 1211 (1997).
5. K. Koynov, S. M. Saltiel, and Y. S. Kivshar, Opt. Lett. **30**, 2284 (2005).
6. S. Zhu, Y. Zhu, and N. Ming, Science **278**, 843 (1997).
7. K. Fradkin-Kashi, A. Arie, P. Urenski, and G. Rosenman, Phys. Rev. Lett. **88**, 23903 (2002).
8. K. R. Parameswaran, R. K. Route, J. R. Kurz, R. V. Roussev, M. M. Fejer, and M. Fujimura, Opt. Lett. **27**, 179 (2002).
9. A. Danielli, P. Rusian, A. Arie, M. H. Chou, and M. M. Fejer, Opt. Lett. **25**, 905 (2000).
10. H.-C. Chui, S.-Y. Shaw, M.-S. Ko, Y.-W. Liu, J.-T. Shy, T. Lin, W.-Y. Cheng, R. V. Roussev, and M. M. Fejer, Opt. Lett. **30**, 646 (2005).
11. R. Klein and A. Arie, Appl. Phys. B **75**, 79 (2002).
12. Yu. N. Korkishko and V. A. Fedorov, in *Ion Exchange in Single Crystals for Integrated Optics and Optoelectronics* (Cambridge International Science, 1999).